Exciton bound to an ionized donor impurity in semiconductor spherical quantum dots

B. Stébé, E. Assaid, F. Dujardin, and S. Le Goff
Laboratoire d'Optoélectronique et de Microélectronique Université de Metz-Institut de Physique-Electronique et Chimie 1 Bd Arago, 57078 Metz Cedex 3, France
(Received 19 July 1996)

The effect of the quantum confinement on the electronic and optical properties of an exciton bound to an ionized hydrogenic donor placed at the center of a semiconductor spherical microcrystal is studied theoretically as a function of the sphere radius R and the effective mass ratio σ of the electron and the hole. The valence- and conduction-band offsets are assumed to be infinite. The ground-state energy is determined by Ritz's variational method. The influence of the confinement on the dipole absorption of the bound exciton is discussed in relation to the exciton absorption. We show that the quantum confinement gives rise to a ''giant'' oscillator strength per impurity, contrary to what happens in bulk materials where a ''giant''oscillator strength results only in the case of a high doping. The ratio between the exciton and the bound-exciton oscillator strengths may be close to unity in small microcrystals, contrary to the three-dimensional case where it is very small. Thus bound-exciton lines are expected to be easier to observe in the former case. [S0163-1829(96)06348-5]

I. INTRODUCTION

The recent progress in crystal growth techniques has made it possible to realize zero-dimensional (0D) systems such as clusters, quantum dots, and microcrystallites. These latter may be present as suspensions in colloidal liquids, or embedded in a glass or rocksalt matrix, with very large energy gaps. In these systems, the ultimate quantum confinement effects restrict the motions of the optically excited electrons and holes in all the three space dimensions. As a consequence, the free particles' energy levels are quantized, and the Coulomb correlation effects and the optical absorption oscillator strengths are enhanced. For more details, we refer the reader to a recent review[1] on the subject. As in the three-dimensional semiconductors, optical excitations may give rise to ''exciton'' (X) or ''bound-exciton'' (BE) states, which must now be interpreted as resonant electronic states of the microcrystals, because there is no longer conservation of the translation motion of the free particles. In 3D semiconductors, the binding energies of BE complexes are generally low, and their existence depends sometimes on specific stability conditions.[2] However, in 0D semiconductors, because the overlapping between the wave functions of the electron and the hole becomes more important, the exciton and BE states are more bound than in the bulk. Moreover, if the confinement potentials may be modeled by an infinitely deep potential well, the possible stability problem no longer occurs because in this case all the particles remain confined in a finite space. So it is expected that the observation of bound excitons should be more easy in 0D semiconductors than in 3D semiconductors.

In the present work we concentrate our study on the (D^+,X) and the (A^-,X) complexes. They result, respectively, from the binding of an exciton to an ionized hydrogenic donor or acceptor impurity. Their possible existence was predicted in 1958 by Lampert.[3] Their stability and binding energies in 3D semiconductors have been the subject of several theoretical studies within the effective mass approximation as a function of the electron to hole effective mass ratio $\sigma = m_e/m_h$. As a result, it appears[4] that the (D^+,X) complex is stable if $\sigma \leqslant \sigma_c = 0.454$ and that the (A^-,X) complex is stable if $\sigma \geqslant \sigma_c$. Up to now, only few theoretical studies have been devoted to the (D^+,X) complex in low-dimensional structures: variational determinations of the ground-state energies in two-dimensional semiconductors[5] and semiconductor quantum wells (QW),[6,7] and a variational-perturbation study in semiconductor microcrystallites.[8]

In this paper we present a fully variational determination of the ground-state energy of the (D^+,X) complex with a hydrogenic donor impurity placed at the center of a semiconductor spherical microcrystallite and determine the oscillator strength for the optical absorption. In Sec. II we present our method of determination of the ground-state energy as well as the absorption coefficient and the oscillator strength. In Sec. III we present and discuss the results of our computations.

II. THEORY

A. Ground-state energy

Let us consider an exciton (X) bound to an ionized hydrogenic donor impurity (D^+) placed at the center of a semiconductor spherical microcrystal embedded in a glassy matrix. We assume that the electron and the hole are completely confined in the microcrystal by an infinite potential barrier. We neglect the effect of the polarization charge induced at the surface. In the case of the effective mass approximation and assuming isotropic parabolic and nondegenerated bands the Hamiltonian of the (D^+,X) complex is written:

$$\mathcal{H} = T + V + V_w + \epsilon_g \equiv H + \epsilon_g . \tag{1}$$

ϵ_g corresponds to the band-gap energy of the bulk semiconductor. Afterwards we use as unit of length the 3D donor effective Bohr radius $a_D = \kappa\hbar^2/e^2 m_e$ and as unit of energy

$\hbar^2/m_e a_D^2$, which represents twice the absolute value of the 3D donor ground-state energy. The dielectric constant κ is introduced in order to take into account the possible polarization effects. The kinetic energy operator T is then given by

$$T=-\frac{1}{2}\Delta_e-\frac{\sigma}{2}\Delta_h\equiv T_e+\sigma T_h, \tag{2}$$

where $\sigma=m_e/m_h$ is the ratio of the effective masses of the electron and the hole. For the ground state, it is sufficient to consider a wave function depending only on the three distances r_e, r_h, and r_{eh}. Within these coordinates, the kinetic energy and Coulomb potential energy operators read

$$T_e=-\frac{1}{r_e}\frac{\partial}{\partial r_e}-\frac{1}{2}\frac{\partial^2}{\partial r_e^2}-\frac{1}{r_{eh}}\frac{\partial}{\partial r_{eh}}-\frac{1}{2}\frac{\partial^2}{\partial r_{eh}^2}-\frac{r_e^2-r_h^2+r_{eh}^2}{2r_e r_{eh}}\frac{\partial^2}{\partial r_e\partial r_{eh}}, \tag{3}$$

$$T_h=-\frac{1}{r_h}\frac{\partial}{\partial r_h}-\frac{1}{2}\frac{\partial^2}{\partial r_h^2}-\frac{1}{r_{eh}}\frac{\partial}{\partial r_{eh}}-\frac{1}{2}\frac{\partial^2}{\partial r_{eh}^2}-\frac{r_h^2-r_e^2+r_{eh}^2}{2r_h r_{eh}}\frac{\partial^2}{\partial r_h\partial r_{eh}}, \tag{4}$$

$$V=-\frac{1}{r_e}+\frac{1}{r_h}-\frac{1}{r_{eh}}. \tag{5}$$

The total confinement potential V_w is written as follows, assuming infinitely deep electron and hole potential wells:

$$V_w=V_{w_e}+V_{w_h}, \tag{6}$$

$$V_{w_i}=\begin{cases}0 & \text{if} \quad r_i<R\\ \infty & \text{if} \quad r_i\geqslant R.\end{cases} \tag{7}$$

The validity of this approximation depends on the conduction- and valence-band offsets as well as on the radius R. In the case of semiconductor microcrystals embedded in a glass matrix, we can assume very large band offsets, so that this approximation is justified for all nonzero R values. In the case of finite band offsets, which corresponds to the case of microcrystals surrounded by another semiconductor, our approximation is justified only in the case of intermediate to small quantum confinement ($R\geqslant 1$ a.u.). In all cases, when R becomes very large, our approximation is expected to lead to the ''exact'' 3D values, depending on the accuracy of our wave function. However, when R tends to zero, this approximation may no longer be used, because it would lead to infinite energy values, whereas a finite potential well would lead to the finite 3D energy values corresponding to the well material. Nevertheless, it must be stressed that for very low R values ($R\leqslant 1-5$ nm), the effective mass approximation becomes unjustified. So, it seems to us that the use of the infinite potential well approximation, which is consistent with the use of the effective mass approximation, and which is expected to lead to reasonable energy values in the case of practical R values, appears to be a good compromise between accuracy and computer time. Indeed, though the use of infinite potential wells does not consistently modify the analytic calculations, it decreases significantly the computer time necessary to compute numerically all of the manifold integrals needed.

The energy and the envelope wave function are solutions of the effective Schrödinger equation:

$$H\Psi=(\epsilon-\epsilon_g)\Psi\equiv E\Psi. \tag{8}$$

This equation is not solvable analytically and we determine its ground-state solutions using Ritz's variational principle. We choose the following trial wave function which generalizes that previously used[5–7] in the study of the (D^+,X) complex in bulk semiconductors, 2D semiconductors, and quantum wells:

$$\Psi=\mathcal{N}\sum_{mnp} c_{mnp}|mnp), \tag{9}$$

$$|mnp)=f_e(r_e)f_h(r_h)\exp(-\alpha r_e-\beta r_{eh})r_e^m r_h^n r_{eh}^p, \tag{10}$$

$$f_e(r)=f_h(r)=j_0(\pi r/R)=\frac{\sin(\pi r/R)}{\pi r/R}, \tag{11}$$

$\mathcal{N}$ stands for the normalization constant. The product $f_e(r_e)f_h(r_h)$ describes the ground state of an uncorrelated electron-hole pair confined in an infinitely deep spherical potential well and j_0 is the zeroth-order spherical Bessel function. The corresponding energy is $E_p=E_e+E_h$, where $E_e=\pi^2/2R^2$ and $E_h=\sigma E_e$ are the ground-state energies of the confined electron and hole, thus $E_p=\pi^2(1+\sigma)/2R^2$. The first exponential factor $\exp(-\alpha r_e)$ describes the Coulombic spatial correlation between the electron and the ionized donor. The second exponential factor $\exp(-\beta r_{eh})$ expresses the Coulombic spatial correlation between the electron and the hole. The integers m, n, and p are positive or equal to zero. The product $r_e^m r_h^n r_{eh}^p$ is introduced in order to take into account the spatial correlations mentioned above. This function is expected to lead to less accurate results when $R\to\infty$ than that used previously[4] in the 3D limit. However, for finite values of R, it appears to be a good compromise between accuracy and computing time.

The linear coefficients c_{mnp} as well as the nonlinear parameters α and β are determined in order to minimize the mean value of the energy:

$$\langle E(\alpha,\beta)\rangle=\langle\Psi|H|\Psi\rangle/\langle\Psi|\Psi\rangle. \tag{12}$$

This leads us, for given values of α and β, to the following system of linear equations:

$$(\mathbf{T}+\mathbf{V}-E\mathbf{S})\mathbf{c}=0, \tag{13}$$

where $\mathbf{T}$, $\mathbf{V}$, and $\mathbf{S}$ represent, respectively, the matrices of the kinetic energy, the Coulomb potential energy, and the norm with respect to the basis functions $|mnp)$. Further, $\mathbf{c}$ denotes the column matrix of the coefficients c_{mnp}. All the matrix elements may be expressed as functions of the following five threefold integrals:

$$I_{mnp}^{m'n'p'}(\lambda,\mu,\nu)=8\pi^2\int_0^R dr_e\int_0^R dr_h\int_{|r_e-r_h|}^{r_e+r_h} dr_{eh} j_0^2(\pi r_e/R) j_0^2(\pi r_h/R)$$
$$\times\exp(-2\alpha r_e-2\beta r_{eh}) r_e^{m+m'+\lambda+1} r_h^{n+n'+\mu+1} r_{eh}^{p+p'+\nu+1},$$

$$J_{mnp}^{m'n'p'}(\lambda,\mu,\nu)=8\pi^2\int_0^R dr_e\int_0^R dr_h\int_{|r_e-r_h|}^{r_e+r_h} dr_{eh} j_0^2(\pi r_e/R) j_0(\pi r_h/R)\cos(\pi r_h/R)$$
$$\times\exp(-2\alpha r_e-2\beta r_{eh}) r_e^{m+m'+\lambda+1} r_h^{n+n'+\mu} r_{eh}^{p+p'+\nu+1},$$

$$K_{mnp}^{m'n'p'}(\lambda,\mu,\nu)=8\pi^2\int_0^R dr_e\int_0^R dr_h\int_{|r_e+r_h|}^{r_e+r_h} dr_{eh} j_0(\pi r_e/R) j_0^2(\pi r_h/R)\cos(\pi r_e/R)$$
$$\times\exp(-2\alpha r_e-2\beta r_{eh}) r_e^{m+m'+\lambda} r_h^{n+n'+\mu+1} r_{eh}^{p+p'+\nu+1},$$

$$L_{mnp}^{m'n'p'}(\lambda,\mu,\nu)=8\pi^2\int_0^R dr_e\int_0^R dr_h\int_{|r_e-r_h|}^{r_e+r_h} dr_{eh} j_0^2(\pi r_e/R) j_0(\pi r_h/R) j_1(\pi r_h/R)$$
$$\times\exp(-2\alpha r_e-2\beta r_{eh}) r_e^{m+m'+\lambda+1} r_h^{n+n'+\mu} r_{eh}^{p+p'+\nu+1},$$

$$M_{mnp}^{m'n'p'}(\lambda,\mu,\nu)=8\pi^2\int_0^R dr_e\int_0^R dr_h\int_{|r_e-r_h|}^{r_e+r_h} dr_{eh} j_0(\pi r_e/R) j_0^2(\pi r_h/R) j_1(\pi r_e/R)$$
$$\times\exp(-2\alpha r_e-2\beta r_{eh}) r_e^{m+m'+\lambda} r_h^{n+n'+\mu+1} r_{eh}^{p+p'+\nu+1}. \quad (14)$$

$j_0(x)=(\sin x)/x$ and $j_1(x)=(\sin x)/x^2-(\cos x)/x$ are the spherical Bessel functions, respectively, of order zero and one. The explicit expressions of all the matrix elements as well as those corresponding to the mean distances are given in the Appendix.

B. Optical properties

It may be interesting to see whether the bound-exciton oscillator strength may be considered as ''giant'' in comparison with the exciton oscillator strength. We consider the optical absorption by a sample of volume Ω_∞ containing identical semiconducting microspheres of volume Ω_m embedded in a matrix transparent in the spectral region $\Delta\omega$ of interest. We assume that the dielectric heterogeneity of the medium has no notable effect on the electromagnetic field of the incident wave and that a given microsphere contains only one sole impurity located at its center. This last assumption is realistic in the case of usual doping rates n_D. Indeed, the mean radius $R_D=(3/4\pi n_D)^{1/3}$ of a sphere containing only one impurity amounts to $R_D=6.2$ nm in the case of a strong doping ($n_D=10^{18}$ cm^{-3}) and to $R_D=133.6$ nm in the case of a weaker doping ($n_D=10^{14}$ cm^{-3}). This last value corresponds to very large microspheres for which the effect of the quantum confinement becomes negligible. So, our hypothesis seems to be justified in the case of microcrystals of usual sizes.

Since the theories of the optical absorption of ionized bound excitons (D^+,X) and free excitons (X) are quite analogous, we present here a common treatment for the two cases. We restrict ourselves to one photon transitions at $T=0$ K between an initial state corresponding to a microcrystal with one ionized impurity D^+ and a final state of an exciton bound to this impurity. For the sake of simplicity, we do not take into account all the details of the band structure.

Generally speaking, the oscillator strength per microsphere for a radiation of circular frequency ω may be defined in relation to the integrated absorption coefficient:

$$f(\omega)=\Omega_\infty\frac{cnm}{2\pi^2}\int_{\Delta\omega}\alpha(\omega')d\omega', \quad (15)$$

where Ω_∞ represents the fundamental volume of normalization of the radiation field, and α is the absorption coefficient per microsphere. Furthermore, c is the velocity of the light in the vacuum, n the index of refraction of the semiconductor, m the mass of the electron at rest, whereas $\Delta\omega$ corresponds to a small interval of frequencies around the transition frequency of interest. We determine the absorption coefficient α per microsphere in a two band model within the effective mass approximation, the dipolar approximation, and neglecting possible nonlinear effects. We obtain

$$\alpha(\omega)=\frac{4\pi^2}{ncm^2\omega\Omega_\infty}\frac{\Omega_m}{\Omega_\infty}\mu^2 I\,\delta(\mathcal{E}_{(D^+,X)}-\mathcal{E}_{D^+}-\hbar\omega), \quad (16)$$

where μ^2 is the square of the interband matrix momentum element at the center of the Brillouin zone. $\mathcal{E}_{(D^+,X)}$ and $\mathcal{E}_{D^+}$ denote the crystal electronic excitation energies corresponding to the initial and final states. We have introduced the dimensionless ''envelope oscillator strength'' defined by

$$I=\left|\int_{\text{sphere}} d^3r_1 d^3r_2\,\Psi(\mathbf{r}_1,\mathbf{r}_2)\,\delta(\mathbf{r}_1-\mathbf{r}_2)\right|^2, \quad (17)$$

which depends only on the normalized envelope wave function Ψ of the exciton or the ionized donor bound exciton. We remark that α is proportional to Ω_m/Ω_∞. In the limit case where the radius of the microsphere tends to infinity, this ratio tends to unity, so that the absorption coefficient becomes identical to the absorption coefficient per impurity that we get in the case of bulk semiconductors[9]. On the other hand, when the radius R tends to zero, this ratio tends also to zero so that the absorption coefficient tends to zero. From Eq. (15) and Eq. (16) it appears that the oscillator strength per microsphere is given by

$$f=\frac{2}{m\hbar\omega_{if}}\mu^2 I, \tag{18}$$

where ω_{if} is the circular frequency corresponding to the given optical transition. It is interesting to remark that, in the effective mass approximation, μ^2 takes the same value for an exciton or an ionized bound-exciton absorption. If we assume that the corresponding transitions energies $\hbar\omega$ are very close, it appears from Eq. (16) and Eq. (18) that the ratio of the absorption coefficient of the ionized donor bound exciton to that of the exciton depends only on the ratio of the corresponding envelope oscillator strengths:

$$\alpha_{(D^+,X)}/\alpha_X=f_{(D^+,X)}/f_X\simeq I_{(D^+,X)}/I_X. \tag{19}$$

Using the variational wave function discussed above, the (D^+,X) envelope oscillator strength reads

$$I_{(D^+,X)}=\left|\frac{4\pi^2}{R^2}\mathcal{N}_{(D^+,X)}\sum_{m,n,p=0}c_{mn0}\int_0^R dr\ r^{m+n+p}\times\exp(-\alpha r)j_0^2(\pi r/R)\right|^2. \tag{20}$$

In order to compare the ionized bound-exciton and the exciton oscillator strengths, it is necessary to evaluate the ratio $f_{(D^+,X)}/f_X\simeq I_{(D^+,X)}/I_X$. For this purpose, we have also determined the exciton envelope oscillator strength I_X using the following wave function:[10,11]

$$\Psi_X=\mathcal{N}_X\exp(-\delta r_{eh})j_0(\pi r_e/R)j_0(\pi r_h/R), \tag{21}$$

where $\mathcal{N}_X$ is a normalization constant and δ a variational parameter. We obtain

$$I_X=(2\pi\mathcal{N}_X R)^2. \tag{22}$$

It can be verified that I_X tends to the expected limit value $\Omega_\infty/\pi(1+\sigma)^3$ when the radius R goes to infinity.

The bound-exciton and exciton transition energies are given by

$$h\nu_{(D^+,X)}=\epsilon_g+E_e+E_h+E^c+\mathcal{E}_0, \tag{23}$$

$$h\nu_X=\epsilon_g+E_e+E_h+E_X^c+\mathcal{E}_0, \tag{24}$$

where we have introduced the ''correlation energies'' defined by

$$E_X^c=E_X-E_e-E_h, \tag{25}$$

$$E^c=E-E_e-E_h, \tag{26}$$

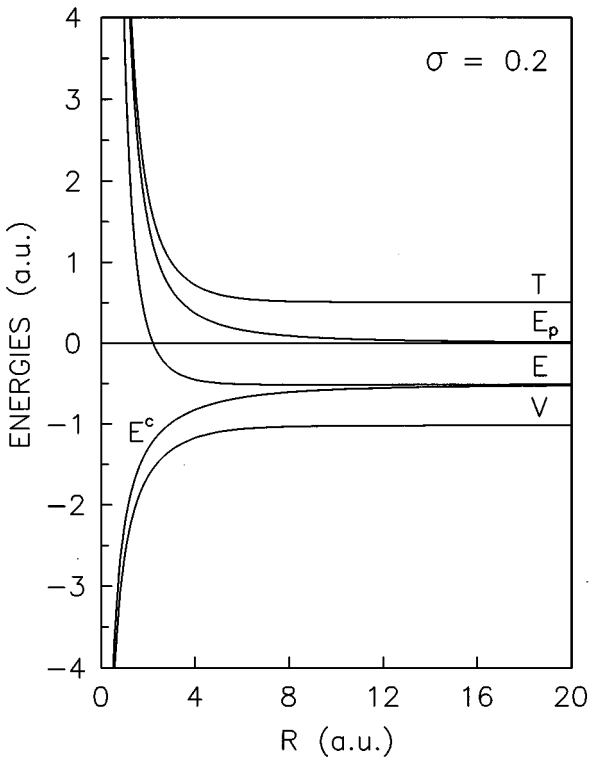

FIG. 1. Total energy E, uncorrelated pair energy E_p, kinetic energy T, Coulomb potential energy V, and correlation energy $E^c=E-E_p$ versus the radius of the spherical crystallite for $\sigma=0.2$.

in relation to the confined electron and hole energies E_e and E_h. $\mathcal{E}_0$ stands for crystal electronic ground-state energy corresponding to full valence bands and empty conduction bands at the temperature $T=0$ K. The localization energy of the bound-exciton lines reads then

$$h\nu_X-h\nu_{(D^+,X)}=E_X^c-E^c. \tag{27}$$

The confinement acts on the positions of the lines associated to the complex and the exciton by shifting them to the high energies.

III. NUMERICAL RESULTS AND DISCUSSION

We have calculated the ground-state energy of the complex as a function of the microcrystallite radius R and the effective mass ratio σ using a ten-term trial wave function defined by the condition $m+n+p\leqslant 2$, which ensures a good accuracy without lengthening the computing time. The integrals have been computed using the 12-term Gauss quadrature method. The energies are estimated to be accurate within six significant figures. Figure 1 shows the variations of the uncorrelated confined pair energy E_p and of the total E, kinetic T, potential V, and correlation E^c mean value energies of the complex as functions of the radius R for $\sigma=0.2$. We remark first that the quantum confinement increases, as expected, the absolute mean value of the Coulomb correlation energy $\langle E^c\rangle$.

In the limit $R\to\infty$, $\langle E^c\rangle\to\langle E\rangle\to-0.51$ a.u., in good agreement with the 3D results.[4,5] Further, $\langle T\rangle\to 0.51$ a.u.,

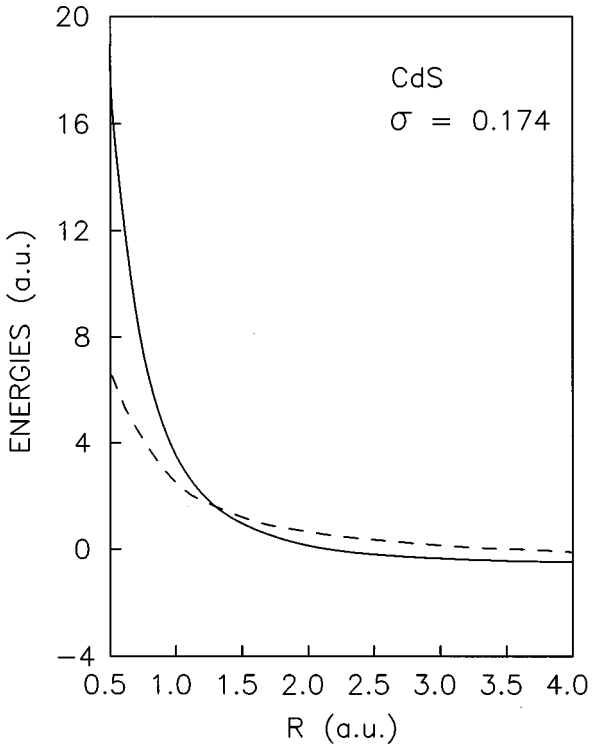

FIG. 2. Comparison between our total energies (solid line) with those obtained by Ping and Dalal (Ref. 8) (dotted line) versus the radius of the microsphere for $\sigma=0.174$, which corresponds to CdS.

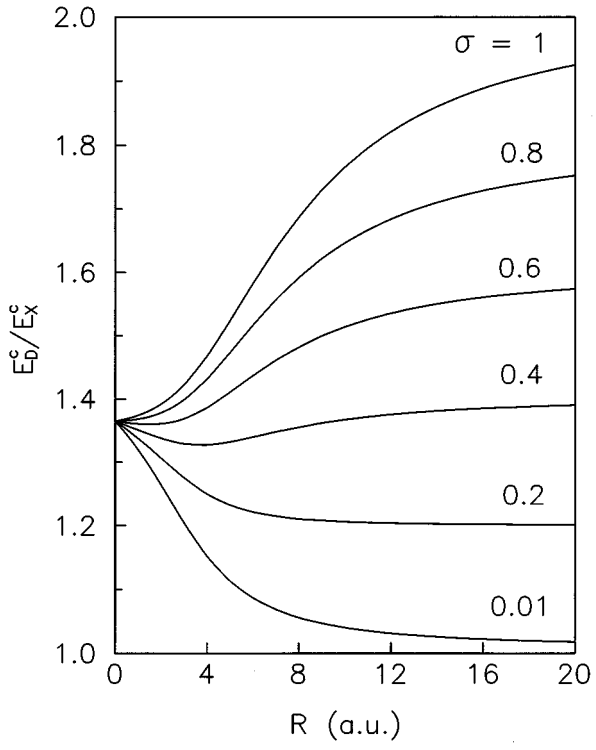

FIG. 3. Ratio of the neutral donor correlation energy to the exciton correlation energy versus the radius of the microsphere for different values of σ.

$\langle V\rangle \rightarrow -1.02$ a.u., so that the virial theorem is satisfied. In the limit $R\rightarrow 0$, the quantum confinement becomes predominant in comparison with the Coulomb interactions. We can estimate the behavior of the mean energies using the asymptotic expression of our trial wave function. In this limit, the terms of the sum in Eq. (9) corresponding to $m+n+p\neq 0$ are expected to give rise to a very small contribution to the total energy of the complex and we may neglect them. Further, we may retain only the first terms of the development near the origin of the exponential part of the wave function, which reduces to

$$\Psi=\exp(-\alpha r_e-\beta r_{eh})j_0(\pi r_e/R)j_0(\pi r_h/R). \quad (28)$$

We obtain the following asymptotic expressions when $R\rightarrow 0$:

$$\langle T\rangle \simeq E_p=\pi^2(1+\sigma)/2R^2,$$

$$\langle V_e\rangle \simeq -\langle V_h\rangle \simeq -K_1/R,$$

$$\langle V_{eh}\rangle \simeq -K_2/R,$$

$$\langle E\rangle \simeq E_p+\langle V_{eh}\rangle,$$

$$\langle E^c\rangle=\langle E\rangle-E_p\simeq\langle V_{eh}\rangle, \quad (29)$$

with $K_1=2.4376$ and $K_2=1.7860$. We remark that in this limit $\langle V_e\rangle=-\langle V_h\rangle$, so that the mean Coulomb potential energy reduces to $\langle V_{eh}\rangle$. Thus we find the same results as previously obtained[11] in the case of a confined exciton, $E_X^c=-1.7860/R$. On the other hand, the neutral donor correlation energy E_D^c reduces to $\langle V_e\rangle=-2.4376/R$ in agreement with a previous result[12]. Finally, we remark that the fact that $\langle E^c\rangle$ varies as $-1/R$ is consistent with our assumption that the electrons and holes are completely confined inside the microsphere.

We can tentatively compare our results with those obtained previously by Ping and Dalal[8] using a variation-perturbation method although this comparison seems to be meaningful only in the limit of large radius, i.e., in the case of a small quantum confinement. Indeed, these authors used a finite confinement potential whereas we have limited ourselves to the case of an infinite potential well. In Fig. 2 we compare the energies obtained by the two methods in the case of CdS microcrystals assuming an effective mass ratio of $\sigma=0.174$. It appears that in the case of intermediate or small confinement ($R>1$ a.u.), our variational method leads, as expected, to better results than the variation-perturbation method. However, in the case of very small microcrystals ($R<1$ a.u.), the energies obtained by Ping and Dalal are better, mainly due to the fact that these authors have used a finite confinement potential. Nevertheless, it must be stressed that in the limit of very small microcrystals the effective mass approximation becomes questionable, so that the comparison of the two methods becomes meaningless in this limit.

Strictly speaking, the problem of the stability of the complex does not exist in a quantum box when assuming an infinite potential well. Indeed, in this case, the ionized donor, the electron, and the hole remain always at finite distances from each other due to the quantum confinement. However, it is well known that in the 3D limit, the complex (D^+,X)

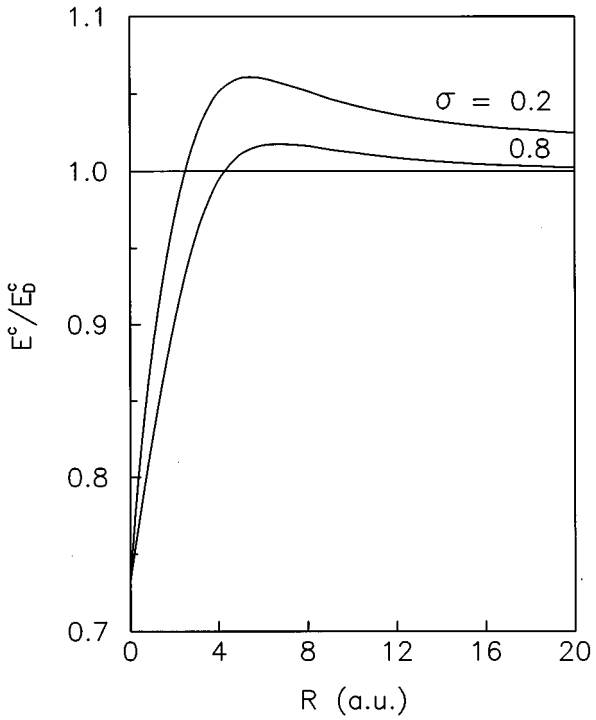

FIG. 4. Ratio of the (D^+,X) correlation energy to the neutral donor correlation energy versus the radius of the microcrystallite for $\sigma=0.2$ and $\sigma=0.8$.

becomes unstable against dissociation into the most stable dissociation product, a neutral donor D^0 and a free hole h with zero kinetic energy,

$$(D^+,X)\rightarrow D^0+h, \tag{30}$$

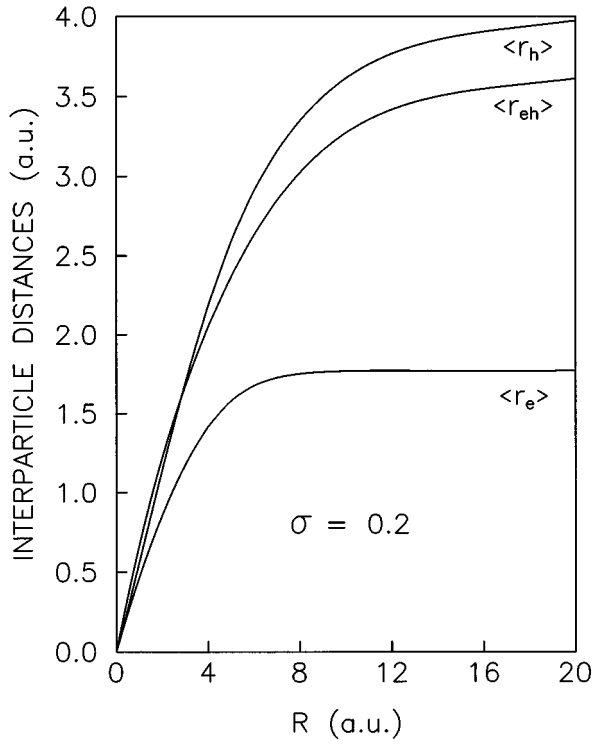

FIG. 5. Spatial extension of the complex drawn against R for $\sigma=0.2$.

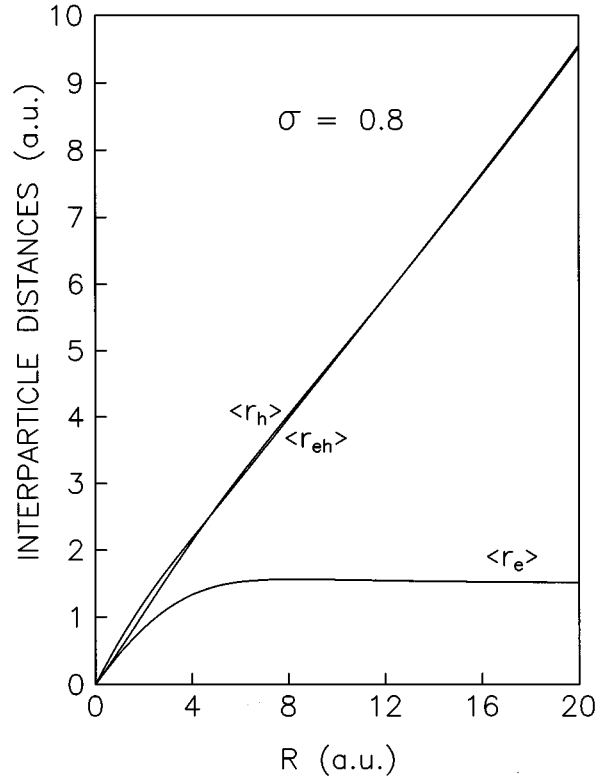

FIG. 6. Spatial extension of the complex drawn against R for $\sigma=0.8$.

because $P(\sigma)=E_D^c/E_X^c>1$ in the 3D limit. The corresponding stability condition may be written

$$E\leqslant E_D+E_h\Leftrightarrow E^c\leqslant E_D^c. \tag{31}$$

In this case, it has been established[4] that the complex remains stable only if $\sigma<\sigma_c\simeq 0.4$. In a microsphere, the dis-

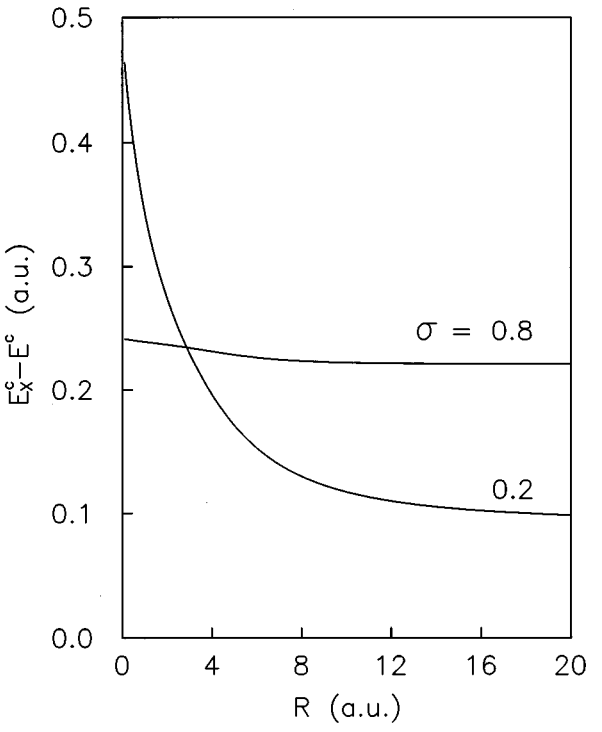

FIG. 7. Localization energy drawn versus the radius R.

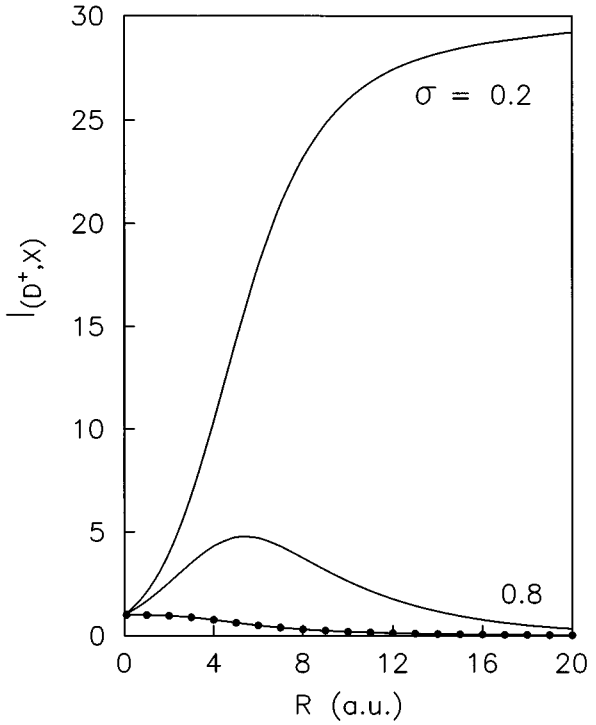

FIG. 8. (D^+,X) envelope oscillator strengths (solid lines) versus the radius R for $\sigma=0.2$ and $\sigma=0.8$. We have also reported the variations of the envelope oscillator strength $I_{(D^0,h)}$ corresponding to a transition towards a noncorrelated neutral donor-hole state (D^0,h) which corresponds to the 3D limit of an unstable (D^+,X) complex.

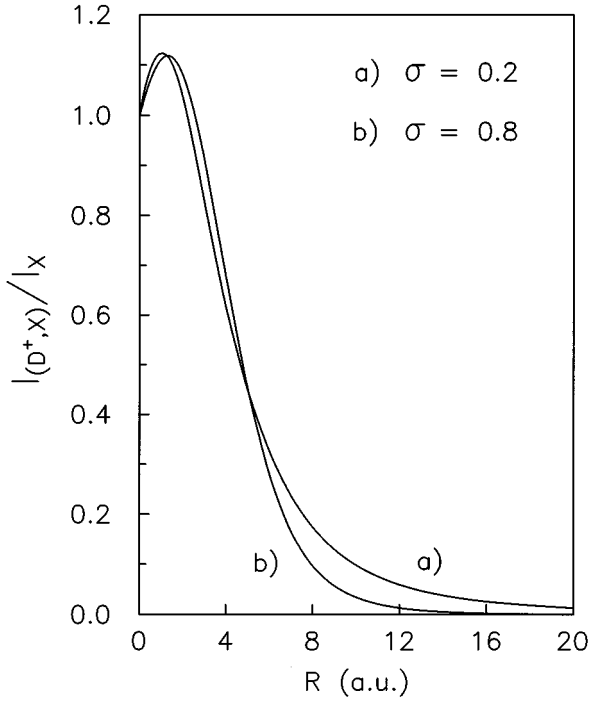

FIG. 9. Ratio $I_{(D^+,X)}/I_X$ drawn against the radius R for $\sigma=0.2$ and $\sigma=0.8$.

cussion about the stability of the complex becomes meaningful only in the limit when $R\to\infty$. We can verify in Fig. 3 that in a microsphere, the above ratio $P(\sigma)=E_D^c/E_X^c$ is also always greater than unity whatever the value of R and of the ratio σ. We remark that when σ tends to zero the ratio $P(\sigma)$ decreases rapidly and becomes very close to unity, which justifies the so-called ''donorlike exciton'' model adopted in the study of the exciton when the hole is infinitely heavy in comparison with the electron. On the other hand, we see that when R tends to zero $P(\sigma)$ tends to the limit 1.3648 independently of σ and when R becomes very large $P(\sigma)$ tends to the expected limit $(1+\sigma)$. These latter results are verified by the study of the asymptotic behaviors of the neutral donor and the exciton inside the microcrystal when the well radius tends to zero and infinity. In Fig. 4 we represent the variations of the ratio E^c/E_D^c as a function of the radius R for $\sigma=0.2$ and $\sigma=0.8$ where the complex is, respectively, stable and unstable in the 3D limit. When $R\to\infty$, for $\sigma=0.2$, $E^c/E_D^c\to1.02>1$, so that we get, as expected, a stable binding. However, for $\sigma=0.8$, $E^c/E_D^c\to1$ which shows that the complex becomes unstable in this limit, like what happens in the 3D case. We remark further that $E^c/E_D^c<1$ for $R\simeq4$ a.u. and that $E^c/E_D^c\to0.7327$ for all values of σ when $R\to0$. This result is consistent with our above discussion. Indeed, following Eq. (29), $E_D^c\simeq-2.4376/R$ and $E^c\simeq-1.786/R$ when $R\to0$. Thus $E^c/E_D^c\to1.786/2.4376=0.7327$ when $R\to0$.

The preceding discussion may be completed by the study of the mean distances between the three particles. We report in Fig. 5 the behavior of the mean values $\langle r_e\rangle$, $\langle r_h\rangle$, and $\langle r_{eh}\rangle$ as functions of the radius R for $\sigma=0.2$. As expected, the three curves converge to zero when R tends to zero while for large R values they tend, respectively, to the limits 1.76, 4.05 and 3.68 a.u. in agreement with the values corresponding to the bulk semiconductor[4]. Fig. 6 shows the variations of $\langle r_e\rangle$, $\langle r_h\rangle$, and of $\langle r_{eh}\rangle$ versus R for $\sigma=0.8$. When R tends to zero, our conclusions are the same as above. However, when R becomes very large, the behavior becomes different. Indeed $\langle r_e\rangle$ tends to 1.50 a.u. units which corresponds to the spatial extension of the neutral donor in bulk semiconductors. On the other hand, $\langle r_h\rangle$ is very close to $\langle r_{eh}\rangle$. The effect of the quantum confinement is now much more important than that of the Coulomb potential. The wave function tends to $j_0(\pi r_h/R)$ from which we may write

$$\langle r_{eh}\rangle\simeq\langle r_h\rangle\simeq\langle j_0(\pi r_h/R)|r_h|j_0(\pi r_h/R)\rangle=R/2. \quad (32)$$

In order to localize the relative position of the complex line we represent in Fig. 7 the variations of $\Delta=h\nu_X-h\nu_{(D^+,X)}$ against the radius R for our two reference values of the ratio σ. We remark that when R tends to zero Δ tends to 0.48 a.u. for $\sigma=0.2$ while it tends to 0.24 a.u. if $\sigma=0.8$. Otherwise $\Delta(R)$ is a decreasing function which tends to the limits 0.09 and 0.22 a.u. for σ equal to 0.2 and 0.8, respectively, from which we may conclude that the confinement increases the localization energy Δ.

In Fig. 8 we report the variations of $I_{(D^+,X)}$ as a function of the radius R for $\sigma=0.2$ and $\sigma=0.8$. In the two cases, when R tends to zero, the confinement potential becomes more important than the Coulomb potential and $I_{(D^+,X)}$ tends to a limit value which corresponds to the envelope oscillator strength of a confined, but noncorrelated, electron-hole pair. For $\sigma=0.2$, $I_{(D^+,X)}$ is an increasing function of R, showing that it is depending, as expected, on the volume available for

the complex. When R tends to infinity, this integral tends to the limit value which has been obtained in the case of bulk semiconductors[4]. For $\sigma=0.8$, $I_{(D^+,X)}$ exhibits a maximum for a radius close to 5 a.u. Below this value, the quantum confinement is predominant and the electron remains close to the hole, so that we observe a similar behavior as for $\sigma=0.2$. However, for $R>5$ a.u., the effect of the quantum confinement becomes negligible with respect to the Coulomb correlation. Because for $\sigma=0.8$ the complex becomes unstable when R goes to infinity, the hole moves far away from the electron so that the envelope oscillator strength decreases at increasing R values.

In the same figure, we have also reported the variations of the envelope oscillator strength $I_{(D^0,h)}$ corresponding to a transition towards a noncorrelated neutral donor-hole state (D^0,h), which corresponds to the 3D limit of an unstable (D^+,X) complex. It can be verified that $I_{(D^0,h)}$ is a strictly decreasing function of R and that for $\sigma=0.8$, $I_{(D^+,X)}$ tends to the same limit as $I_{(D^0,h)}$ when R goes to infinity. We may compare the above results with those obtained recently by Ping and Dalal.[8] They obtained an envelope oscillator strength $I_{(D^+,X)}$ which decreases with R and which does not tend towards the expected limit when R tends to infinity. This behavior is comparable with that of the envelope oscillator strength $I_{(D^0,h)}$ of the (D^0,h) state that we have discussed above. This discrepancy with our results is due to the fact that these authors have treated the Coulomb electron-hole interaction as a perturbation, which is only justified for very small R values.

Figure 9 shows the variations of the ratio $I_{(D^+,X)}/I_X$ as a function of R for the same two values of σ we used above. We remark first that its behavior is quite analogous in the two cases. When R goes to zero, the two oscillator strengths become identical. This is due to the fact that in this limit the effect of the Coulomb correlation effect becomes negligible in comparison with that of the quantum confinement. At increasing R, the ratio increases towards a maximum value $I_{(D^+,X)}/I_X\simeq 1.1$, corresponding to $R\simeq 2$ a.u. In this case, the ionized donor bound-exciton oscillator strength is greater than the exciton oscillator strength, showing that the effect of the quantum confinement on the Coulomb interaction is more important in the case of the ionized donor bound exciton. However, when R tends to infinity, the ratio becomes very small, and the exciton oscillator strength becomes much higher than the ionized bound-exciton oscillator strength, and we cannot at all speak about a giant oscillator strength per impurity for the (D^+,X) complex, contrary to what has been claimed many years ago.[13,14] On the other hand, it is clear that our assumption on one sole impurity per microsphere becomes questionable when R tends to infinity, because it corresponds to a very small doping.

In reality, it is easy to show that in the case of bulk semiconductors, the ionized donor bound-exciton envelope oscillator strength per impurity is very small compared to that of the exciton, provided that the two oscillator strengths are determined with reference to the same volume. However, a large bound-exciton oscillator strength may result from a large doping and not from a giant envelope oscillator strength per impurity. Indeed, in the 3D limit, we obtain, in the case of a crystal of volume Ω_∞ containing N_D impurities,

$$f_{(D^+,X)}/f_X\simeq n_D I^{3D}_{(D^+,X)}\pi a_X^3, \tag{33}$$

where $n_D=N_D/\Omega_\infty$ is the impurity concentration and where we have assumed, as above, that $\hbar\omega_X/\hbar\omega_{(D^+,X)}\simeq 1$. This ratio becomes very small when the impurity concentration n_D becomes very low, provided that $I^{3D}_{(D^+,X)}$ and a_X remain finite. For example, for $\sigma=0.2$, using the 3D value $I^{3D}_{(D^+,X)}\simeq 30$ obtained previously,[4] we get $I^{3D}_{(D^+,X)}\pi a_X^3\simeq 10^{-16}$ cm^3 with $a_X\simeq 100$ Å. The ratio of the bound exciton to the exciton envelope oscillator strengths is thus not at all giant, but can be very low, in agreement with our above results. It is important to remark that the value of the ratio of the oscillator strengths, Eq. (33), is proportional to the impurity concentration n_D. For example, at low doping with $n_D\simeq 10^{14}$ cm^{-3}, $f_{(D^+,X)}/f_X=10^{-2}$. At high doping with $n_D\simeq 10^{18}$ cm^{-3}, $f_{(D^+,X)}/f_X=10^2$. Crudely speaking, in bulk semiconductors, large oscillator strength can only occur when the number of impurities per unit volume is large in comparison with the number of excitons per unit volume, or in other words, when a large number of unit cells are doped.

The reason why in the past it has been claimed that excitons weakly bound to impurities exhibit giant oscillator strengths, independently from the impurity concentration, arises from the fact that Rashba and Gurgenishvili[13,14] compared two oscillator strengths not corresponding to the same crystal volume. He compared the ionized bound-exciton oscillator strength per impurity for the whole crystal to the exciton oscillator strength per unit cell and obtained the following ratio:

$$f^{\rm imp}_{(D^+,X)}/f^{\rm UC}_X=I^{3D}_{(D^+,X)}\pi a_X^3/\Omega_0, \tag{34}$$

where $\Omega_0=\Omega_\infty/N$ is the volume of the unit cell of the crystal containing N unit cells. For example, in a cubic material, $\Omega_0=a^3$, where the lattice constant a is typically of the order of $a=5$ Å. Assuming the same 3D envelope oscillator strength $I^{3D}_{(D^+,X)}\simeq 30$, and exciton Bohr radius $a_X\simeq 100$ Å as above, the ratio of Eq. (34) amounts then to 7×10^5, which appears to be giant. But it must be stressed that this ratio is not significant because the two oscillator strengths do not refer to the same volume. This ratio becomes meaningful only in the limit case where each unit cell is doped with one impurity. In this case, $N_D=N=\Omega_\infty/\Omega_0$ and the impurity concentration becomes $n_D=N_D/\Omega_\infty=1/\Omega_0=1/a^3$. In the case of a cubic crystal with $a=5$ Å, this corresponds to a very giant impurity concentration $n_D=8\times 10^{21}$, which indeed is not very realistic.

Therefore we have shown that in a microsphere, due to the quantum confinement, the envelope bound-exciton oscillator strength may be considered as giant in comparison to what we get in bulk semiconductors. In particular, we expect that even with only one sole impurity per microsphere, the intensities of the (D^+,X) and the exciton lines should have comparable intensity if $R\simeq 2$ a.u., i.e., $R\simeq 100$ Å. As a consequence, we expect that the observation of ionized bound excitons should be more easy in low-dimensional microcrystals than in bulk semiconductors. Nevertheless, this conclusion should be moderated by the fact that a giant oscillator strength does not necessarily lead to a giant total absorption coefficient. Indeed, if the sample contains identical semiconducting microspheres, and if only a fraction τ $(0\leqslant\tau\leqslant 1)$ of the microspheres is doped with one sole impurity, the ratio of the total absorption coefficients becomes

$$\alpha_{(D^+,X)}/\alpha_X = \tau f_{(D^+,X)}/f_X \simeq \tau I_{(D^+,X)}/I_X \tag{35}$$

and may become small when not enough microspheres are doped.

To conclude, we remark that all the above results may be used without difficulties to get some insight into the properties of another kind of exciton-ionized impurity complex: the exciton-ionized acceptor complex (A^-,X). Indeed, within the effective mass approximation and assuming infinitely deep confinement potentials, it is easy to verify that the following relation holds:

$$\frac{E_{(A^-,X)}(\sigma)}{E_{A^0}} = \frac{E_{(D^+,X)}(1/\sigma)}{E_{D^0}}. \tag{36}$$

APPENDIX: MATRIX ELEMENTS

In order to determine the matrix elements between the states $|i\rangle \equiv |mnp\rangle$ and $|i'\rangle \equiv |m'n'p'\rangle$, we define

$$I_{ii'}(\lambda,\mu,\nu) = I(\lambda,\mu,\nu), \tag{A1}$$

$$J_{ii'}(\lambda,\mu,\nu) = J(\lambda,\mu,\nu), \tag{A2}$$

$$K_{ii'}(\lambda,\mu,\nu) = K(\lambda,\mu,\nu), \tag{A3}$$

$$L_{ii'}(\lambda,\mu,\nu) = L(\lambda,\mu,\nu), \tag{A4}$$

$$M_{ii'}(\lambda,\mu,\nu) = M(\lambda,\mu,\nu). \tag{A5}$$

So we get

$$S_{ii'} = I(0,0,0), \tag{A6}$$

$$T_{ii'} = T^e_{ii'} + \sigma T^h_{ii'}, \tag{A7}$$

$$\begin{aligned} T^e_{ii'} = &-\frac{m(m-1)}{2} I(-2,0,0) - \frac{p(p+m)}{2} I(0,0,-2) + \frac{\alpha(2m+p)}{2} I(-1,0,0) + \frac{\beta(2p+m+1)}{2} I(0,0,-1) \\ &+ \frac{\pi^2-\alpha^2R^2-\beta^2R^2}{2R^2} I(0,0,0) - \frac{\beta\alpha}{2} I(-1,0,1) - \frac{\beta\alpha}{2} I(1,0,-1) + \frac{\beta\alpha}{2} I(-1,2,-1) + \frac{\alpha p}{2} I(1,0,-2) - \frac{\alpha p}{2} I(-1,2,-2) \\ &- \frac{mp}{2} I(-2,0,0) + \frac{mp}{2} I(-2,2,-2) + \frac{m\beta}{2} I(-2,0,1) - \frac{m\beta}{2} I(-2,2,-1) - \frac{m\pi}{R} K(-1,0,0) + \frac{\alpha\pi}{R} K(0,0,0) \\ &- \frac{p\pi}{2R} K(1,0,-2) + \frac{\beta\pi}{2R} K(1,0,-1) - \frac{p}{2} M(0,0,0) + \frac{p}{2} M(0,2,-2) + \frac{\beta}{2} M(0,0,1) - \frac{\beta}{2} M(0,2,-1), \end{aligned} \tag{A8}$$

$$\begin{aligned} T^h_{ii'} = &-\frac{n(n-1)}{2} I(0,-2,0) - \frac{p(p+n)}{2} I(0,0,-2) + \frac{\beta(2p+n+1)}{2} I(0,0,-1) + \frac{\pi^2-\beta^2R^2}{2R^2} I(0,0,0) - \frac{np}{2} I(0,-2,0) \\ &+ \frac{np}{2} I(2,-2,-2) + \frac{n\beta}{2} I(0,-2,1) - \frac{n\beta}{2} I(2,-2,-1) - \frac{\pi}{R} J(0,-1,0) - \frac{p\pi}{2R} J(0,1,-2) + \frac{\beta\pi}{2R} J(0,1,-1) \\ &- \frac{p}{2} L(0,0,0) + \frac{p}{2} L(2,0,-2) + \frac{\beta}{2} L(0,0,1) - \frac{\beta}{2} L(2,0,-1), \end{aligned} \tag{A9}$$

$$V_{ii'} = -I(-1,0,0) + I(0,-1,0) - I(0,0,-1). \tag{A10}$$

In the same way the matrix elements for the mean distances are given by

$$r^e_{ii'} = I(1,0,0), \tag{A11}$$

$$r^h_{ii'} = I(0,1,0), \tag{A12}$$

$$r^e_{ii'} = I(0,0,1). \tag{A13}$$

[1] A.D. Yoffe, Adv. Phys. **42**, 173 (1993).

[2] P.J. Dean and D.C. Herbert, in *Excitons*, edited by K. Cho, Topics in Current Physics Vol. 14 (Springer-Verlag, Berlin, 1979), p. 55.

[3] M.A. Lampert, Phys. Rev. Lett. **1**, 450 (1958).

[4] T. Skettrup, M. Suffczynski, and W. Gorzkowski, Phys. Rev. B **4**, 512 (1971).

[5] B. Stébé and L. Stauffer, Superlatt. Microstruct. **5**, 451 (1989).

[6] L. Stauffer and B. Stébé, Solid State Commun. **80**, 983 (1991).

[7] B. Stébé, L. Stauffer, and D. Fristot, J. Phys. (France) IV **3**, C5-417 (1993).

[8] E.X. Ping and V. Dalal, Solid State Commun. **82**, 749 (1992).

[9] L. Stauffer, B. Stébé, and G. Munschy, Phys. Status Solidi B **119**, 193 (1983).

[10] Y. Kayanuma, Solid State Commun. **59**, 405 (1986).

[11] Y. Kayanuma, Phys. Rev. B **38**, 9797 (1988).

[12] A.I. Ekimov, I.A. Kudryavtsev, M.G. Ivanov, and Al. L. Efros, Fiz. Tverd. Tela (Leningrad) **31**, 192 (1989) [Sov. Phys. Solid State **31**, 1385 (1989)].

[13] E.I. Rashba and G.E. Gurgenishvili, Fiz. Tverd. Tela (Leningrad) **4**, 1029 (1962) [Sov. Phys. Solid State **4**, 759 (1962)].

[14] E.I. Rashba, Fiz. Tekh. Poluprovodn. **8**, 1241 (1974) [Sov. Phys. Semicond. **8**, 807 (1975)].